Vietnam Journal of Mechanics, VAST, Vol. 44, No. 2 (2022), pp. 117 – 132
DOI: https://doi.org/10.15625/0866-7136/16696

GRAVITY-DRIVEN WET GRANULAR FREE-SURFACE FLOWS DOWN AN INCLINED PLANE: EFFECTS OF THE INCLINATION ANGLE

Thanh-Trung Vo[1,2,*], **Trung-Kien Nguyen**[3], **Cuong T. Nguyen**[4,5]
[1]*School of Transportation Engineering, Danang Architecture University, 566 Nui Thanh street, Da Nang City, Vietnam*
[2]*Office of Research Administration, Danang Architecture University, 566 Nui Thanh street, Da Nang City, Vietnam*
[3]*Faculty of Building and Industrial Construction, Hanoi University of Civil Engineering, 55 Giai Phong Road, Hanoi, Vietnam*
[4]*Faculty of Vehicle and Energy Engineering, Phenikaa University, Hanoi, Vietnam*
[5]*Phenikaa Research and Technology Institute (PRATI), 167 Hoang Ngan street, Cau Giay district, Hanoi, Vietnam*
[*]E-mail: trungvt@dau.edu.vn

Received: 07 November 2021 / Published online: 22 May 2022

Abstract. Wet granular materials flowing down an inclined plane are omnipresent in multi-field engineering. Although extensive research has been carried out to investigate the flowability of such flows, our understanding of the flows like landslides is limited due to the presence of the cohesive forces between particles and the arbitrarity of inclination angle. In this paper, we explore the effects of the inclination angle on the velocity profiles and force distribution of the gravity-driven wet granular free-surface flows in the steady-flowing state by means of an extensive discrete element method with the inclusion of the capillary cohesion law. This capillary cohesion law is enhanced by the capillary attraction force due to the presence of the liquid bridges between near-neighboring particles. The results show that the mobility of wet granular materials is strongly controlled by the inclination angle due to the domination of the gravity effects of particles as compared to the cohesion effects and rough effects of the inclined surface. These observations are consistent with the previous experimental work done on the granular collapse on an inclined plane. Furthermore, in its steady-state flow, the granular materials separate stably into two different flowing regions: solid-like and fluid-like flows, and the depth of these flows strongly depends on the values of the inclination angle. More interestingly, the inclination angle also strongly governs the density and intensity of the tensile and compressive components of the normal forces and tangential forces in both solid-like and fluid-like regions with different characteristics.

Keywords: capillary bridge, discrete element method, force distribution, fluid-like, granular flow, solid-like.

1. INTRODUCTION

Wet granular materials flowing down an inclined plane are omnipresent in geotechnical engineering such as landslides and rock avalanches [1–3]. Characteristics of such flows strongly depend on the particles' gravity, friction coefficient, the inclination angle, the height of the granular column, the rough base, and the cohesion forces between neighboring particles [4–9]. Once occurred, the granular materials start flowing down from the quasi-static regime mainly due to the exceeding of the gravity effects as compared to the frictional effects. The flows then evolve into the inertial regime as a consequence of having the large displacements of granular materials before reaching a steady-flowing state [10–12]. Unlike the dry granular flows, the velocity profiles of granular materials in the steady-flowing state are almost homogeneous which represents the Bagnold velocity profile [13], the gravity-driven wet granular free-surface flows tend to separate stably into two different regions: solid-like and fluid-like [3, 14–17]. In particular, a solid-like flow occurs near the free surface of the flow and its local shear rate is nearly zero, meanwhile, the fluid-like layer appears below the solid-like layer with a large local shear rate [15–18]. Besides the inherent effects of the particles' gravity, friction coefficient, and the interactions between grains, both solid-like and fluid-like layers may strongly depend on the inclination angle. And although extensive studies have been constructed to investigate the rheological properties of gravity-driven dry and wet granular free-surface flows, the fundamental understanding of the underlying physical properties of wet granular materials flowing down an inclined plane is due to the effects of the inclination angle is still limited.

Indeed, a number of the gravity-driven granular free-surface flows have been carried out to investigate their rheological properties and the behavior of the solid-like and fluid-like layers over the last few decades [3, 15, 18–20]. Silbert et al. [19] firstly discussed the formation and the evolution of the solid-like (plug) flow of granular materials flowing down an inclined plane. Brewster and co-workers [18] then numerically measured the effects of the cohesion between grains on the thickness of the solid-like flowing region as well as proposed the modification of the Bagnold prediction of the velocity profiles in the steady-flowing state. Rognon et al. [15] also illustrated the development of the plug region (solid-like flow) from the free surface of granular flow where the cohesion is strongest as compared to the particles' gravity, they also then analyzed the microstructure of the whole flows by measuring the coordination number and the normal forces distribution. Mandal and co-workers [16] numerically highlighted the flowability of cohesive granular media flowing down an inclined plane with a given inclination angle, their results showed the rheological properties of such flows can be described by using an effective cohesion number that incorporates the interparticle cohesion and the

mechanical properties of raw particles. The ordered/disordered behavior of such flows was also discussed by Moharamkhani et al. [17] due to the occurrence and development of the solid-like flow as a consequence of considering the smooth and rough inclined planes. However, most of the investigations above only reported the existence of the solid-like and fluid-like regions but without considering in detail the fundamental mechanism and properties of these flow regions. More interestingly, Zhu and co-workers [3] recently studied the behavior of the solid-like and fluid-like granular flows under the surface-normal vibration. They reported in detail the velocity profiles and the stress distribution for a given inclination angle. However, the effects of the inclination angle on the compressive and tensile forces distribution were also absent.

In this paper, we report in detail the effects of the inclination angle on the velocity profiles and the tensile and compressive forces distribution of the gravity-driven wet granular flowing down an inclined plane by using the three-dimensional discrete element method. The numerical method with the inclusion of the capillary attraction law enhanced by the cohesive and viscous forces that occurred between near-neighboring particles with the presence of the capillary bonds. The sample model is first prepared by using isotropic compaction in a box, the lateral walls of this sample are then replaced by setting the periodic boundary conditions, whereas the bottom wall is replaced by using a rough wall that is defined by gluing monodisperse granular particles. In all the steps above, the gravitational acceleration is activated in the directions perpendicular to the rough bottom wall. After reaching the equilibrium state, three different values of the inclination angle are applied to investigate the flowability of wet granular materials. The results obtained in our paper represent the different effects of the inclination angle on the velocity profiles and force distribution in the solid-like and fluid-like layers.

The rest of our paper is arranged as follows. We first introduce the discrete element method, the model setting, and the key parameters in Section 2. The paper then analyzes the flowability of gravity-driven wet granular free-surface flows down an inclined plane by varying the rough inclination angle in Section 3. The conclusion is set in Section 4 with the salient results and further research directions.

2. NUMERICAL METHOD AND MODEL SETTING

2.1. Discrete element method

The discrete element method (DEM) is extensively used for the simulations of granular materials which are omnipresent in nature, industrial processes, multi-field engineering, and the daily life [21–23]. In DEM, all particles are assumed to be rigid, and each particle interacts with others via the frictional elastic force laws [24,25]. The solid interaction

forces involve the normal contact forces and the tangential contact forces [21,22,24,26]. These normal and tangential forces are proportional to the relatively normal and tangential displacement obtained by using the stepping integration based on the Newton second law [21,22,24,27,28]. The equations of motion of a particle i with its radius R_i are obtained by adding all forces exert on the particle, as given following

$$\begin{aligned} m_i \frac{\mathrm{d}^2 \mathbf{r}_i}{\mathrm{d}t^2} &= \sum \left[\left(f_n^{ij} + f_c^{ij} + f_v^{ij} \right) \mathbf{n}^{ij} + f_t^{ij} \mathbf{t}^{ij} \right] + m_i \mathbf{g}, \\ \mathbf{I}_i \frac{\mathrm{d}\boldsymbol{\omega}_i}{\mathrm{d}t} &= \sum f_t^{ij} \mathbf{c}^{ij} \times \mathbf{t}^{ij}, \end{aligned} \tag{1}$$

where m_i, $\mathbf{r}_i$, I_i, and $\boldsymbol{\omega}_i$ are the mass, position, inertia matrix, and angular velocity of particle i, respectively. j is a near-neighboring particle in contact with particle i. $\mathbf{g}$ denotes the gravitational acceleration vector. $\mathbf{n}^{ij}$ and $\mathbf{t}^{ij}$ are the unit vectors between particle i and j in the normal and tangential directions, respectively. Meanwhile, the normal unit vector has the direction from particle j to particle i, the tangential unit vector has the direction opposite to the relatively tangential displacement between these two particles, as shown in Fig. 1(a). $\mathbf{c}^{ij}$ is an unit vector that pointing from the center of particle i to the contact point with particle j.

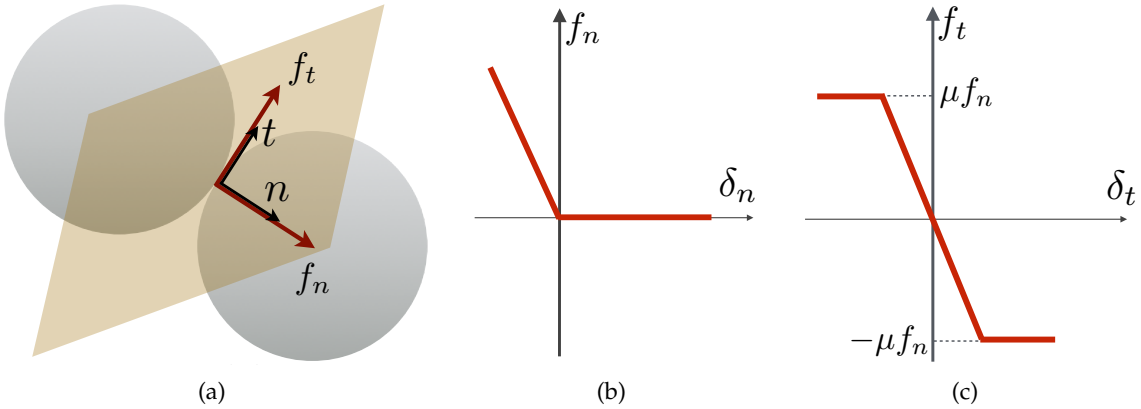

Fig. 1. (a) Local geometry between two particles in solid contact, (b) the normal contact force f_n as a function of the deflection δ_n, and (c) the tangential contact force f_t as a function of the relative tangential displacement δ_t with the Coulomb friction threshold μf_n, where μ is the coefficient of friction

In Eq. (1), the normal contact force f_n and tangential contact force f_t are calculated by using the Signorini model and the Coulomb friction law, respectively. Concerning a normal contact force, it only appears when occurring the overlaps between particles in contacts (Fig. 1(b)), and this force involves two different components: the normal elastic force $f_n^e = k_n \delta_n$ and normal damping force $f_n^d = \gamma_n \dot{\delta}_n$, where k_n and γ_n are the normal

stiffness and normal damping parameter of particle i, δ_n and $\dot{\delta}_n$ denote the deflection and relatively normal velocity between particle i and particle j [21,22,29,30].

The tangential contact force f_t is determined according to the Coulomb friction law, this force is a minimum of two components: the sum of the tangential elastic component $k_t\delta_t$ and tangential viscous damping force $\gamma_t\dot{\delta}_t$ and the threshold of the frictional contact force μf_n, as shown in Fig. 1(c).

$$f_t = -\min\left\{(k_t\delta_t + \gamma_t\dot{\delta}_t), \mu f_n\right\}, \tag{2}$$

where k_t and γ_t denote the tangential elastic stiffness and tangential viscous damping parameter. δ_t and $\dot{\delta}_t$ are the relative tangential displacement and the relative tangential velocity, respectively, between particle i and particle j, μ denotes the coefficient of friction between particles in contact [31–33].

In cohesive granular materials, besides the normal and tangential contact forces that appear in the solid interactions between particles, the interactions between grains are also enhanced by the capillary cohesion forces f_c and viscous forces f_v due to the presence of the capillary bonds of the liquid [33–35], as shown in Fig. 2. In these simulations, the capillary bridges are assumed to be reformed during the flows of granular materials.

The normal capillary attraction force f_c is proportional to the liquid volume V_b of the capillary bonds, the liquid-vapor surface tension γ_s, and the solid-liquid-contact angle θ. In this current work, the angle θ is set to zero due to the fully covering of the liquid on the particle surface. As an approximate solution of the Laplace–Young equation, the cohesion force f_c is determined as following [36]

$$f_c = \begin{cases} -\kappa\, R, & \text{for } \delta_n < 0, \\ -\kappa\, R\, e^{-\delta_n/\lambda}, & \text{for } 0 \le \delta_n \le d_{rupt}, \\ 0, & \text{for } \delta_n > d_{rupt}, \end{cases} \tag{3}$$

where $\kappa = 2\pi\gamma_s \cos\theta$ is the pre-factor of the capillary attraction forces. $R = (R_i R_j)^{1/2}$ is the mean radius of particle i and particle j. d_{rupt} is the rupture distance between particle i and j depending on the volume of the capillary bridge [37], as given by

$$d_{rupt} = \left(1 + \frac{\theta}{2}\right) V_b^{1/3}. \tag{4}$$

As shown in Eq. (3), the capillary attraction force f_c decreases exponentially as a function of the separation distance δ_n between particle i and j in contact. This decrease is characterized by the characteristic length λ, expressed as a function of V_b and $R' = 2R_iR_j/(R_i + R_j)$ [38]

$$\lambda = c\, h(r) \left(\frac{V_b}{R'}\right)^{1/2}, \tag{5}$$

where $r = \max\{R_i/R_j; R_j/R_i\}$ defined as a ratio between two the diameter of particle i and particle j, $h(r) = r^{-1/2}$, and $c \simeq 0.9$ [39].

The viscous force f_v depends on the particle size R, the liquid viscosity η of the capillary bridges, and the relative normal velocity v_n between particles i and j [33,40], as given following

$$f_v = \begin{cases} \frac{3}{2}\pi R^2 \eta \frac{v_n}{\delta_0}, & \text{for } \delta_n \leq 0, \\ \frac{3}{2}\pi R^2 \eta \frac{v_n}{\delta_n + \delta_0}, & \text{for } 0 < \delta_n \leq d_{rupt}, \\ 0, & \text{for } \delta_n > d_{rupt}, \end{cases} \tag{6}$$

where δ_0 is the characteristic length of the particle roughness.

2.2. Model setting and parameters

In order to create the sample of granular materials flowing down an inclined plane, the sample is first prepared by using isotropic compaction of nearly 20,000 spherical particles inside a box under the action of confining stress. This step tends to change the packing of granular particles from a loose configuration to dense one. After that, all the lateral walls of the box are removed and replaced by the periodic boundary conditions, the bottom wall is also removed and replaced by the rough wall that is glued by monodisperse particles, and the gravity of all particles is also activated in the direction that is perpendicular to the rough bottom wall in this current step. This sample is then subjected to the gravity-driven wet granular free-surface flowing down an inclined plane by activating three different values of the inclination angle of the gravitational acceleration vector, as shown in Fig. 2.

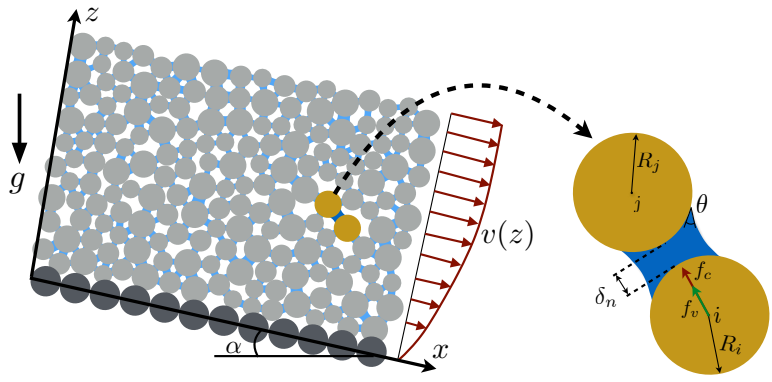

Fig. 2. Schematic drawing representation the gravity-driven wet granular materials free-surface flows down an inclined plane with the inclination angle α and the model of the capillary bridge between two particles i and j in a collection of particles. Red arrows represent the common velocity profile for dense granular flows on an inclined plane

In this simulation model, the particle diameter is varied in a range $[d_{\min}, d_{\max}]$, where $d_{\max} = 2 \times d_{\min}$. The particle size is assumed to be distributed uniformly by particle volume fraction, this tends to avoid the crystallization of granular materials and the ordered dense granular flows. In this current work, the coefficient of friction of particles is set to 0.4, the time step is set to 1.2×10^{-7} sec., this time step is small enough in order to correctly integrate the particle interactions. The inclination angle α is chosen following the experimental work reported by Pouliquen [1], which is large enough in order to generate the flow. All other parameters are reused from our previous work in simple shear flows of unsaturated granular materials [30]. These key parameters are given in Table 1.

Table 1. Main parameters and their values of all simulations

Parameter	Symbol	Value	Unit
Largest particle diameter	$d_{\max}$	1600	µm
Density of particles	ρ	2600	kg.m^{-3}
Number of grains	N_g	19,628	-
Friction coefficient	μ	0.4	-
Normal stiffness	k_n	10^6	N/m
Tangential stiffness	k_t	8×10^5	N/m
Normal damping	γ_n	0.5	Ns/m
Tangential damping	γ_t	0.5	Ns/m
Contact angle	θ	0.0	deg.
Liquid viscosity	η	200.0	mPa.s
Cohesion stress	σ_c	117.52	Pa
Inclination angle	α	$\{23, 25, 27\}$	deg.
Time step	Δt	1.2×10^{-7}	sec.

3. GRAVITY-DRIVEN WET GRANULAR FREE-SURFACE FLOWS

3.1. Flowability of wet granular materials

To investigate the flowability of wet granular materials flowing down an inclined plane, the evolution of the kinetic energy during the flows and the velocity profiles of granular materials in the steady-flowing state are considered. Figs. 3(a) and (b) show the evolution of the normalized mean kinetic energy $\langle E \rangle = \langle mv^2/2 \rangle$ and the free-fall kinetic energy of particles $\langle m \rangle \langle d \rangle / 2g$ during the flows and the evolution of the normalized kinetic energy as a function of the inclination angle α of the plane, respectively, where $\langle m \rangle$

and v are the mean mass and velocity of granular materials, $\langle d \rangle$ is the mean particle diameter, and g denotes the gravitational acceleration. As shown in Fig. 3(a), this energy first increases very slightly at the beginning of the flows when activating the inclination angle of the gravitational acceleration, leading to the occurrence of the solid-like flow in the whole system. The kinetic energy then increases exponentially over time (as a transient state) before reaching the steady-flowing state. In the transient state, the fluid-like layer occurs and develops, leading to decrease of the depth of the solid-like layer. In this current work, the sample model is divided into 20 layers, i.e. with all layers having the same height. The boundary line marks the end of the solid-like region if the velocity in this region is larger than 5% as compared to a layer just below this line. Both the solid-like and fluid-like regions are stable in the steady-flowing state of gravity-driven wet granular free-surface flows. It is also interesting to see that the kinetic energy increases exponentially with increasing the inclination angle α, as shown in Fig. 3(b). As clearly known that the flowability of the gravity-driven granular flow on an inclined plane is mainly governed by the balance between the frictional force exerted at the plane surface and the gravity force induced by the inclination angle [1]. Thus, although the inclination angle α increases slightly from 23 to 27 deg., the flowability characterized by the kinetic energy increases significantly as a consequence of keeping a constant roughness of the plane surface. This observation is consistent with the previous experimental results reported by Pouliquen when considering the kinetic energy of the flow induced by granular collapse on an inclined plane in the steady-state [1].

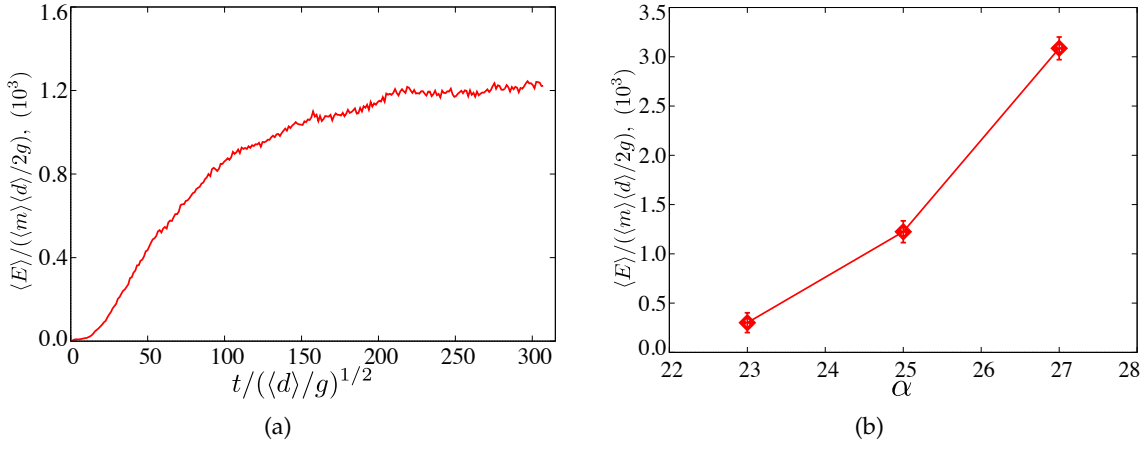

Fig. 3. (a) Evolution of normalized mean kinetic energy of granular flows by the free-fall energy of the particle having the mean diameter for the case of the inclination angle $\alpha = 25$ deg. from the static regime to the inertial regime, (b) variation of this normalized mean kinetic energy as a function of the inclination angle α in the steady-flowing state

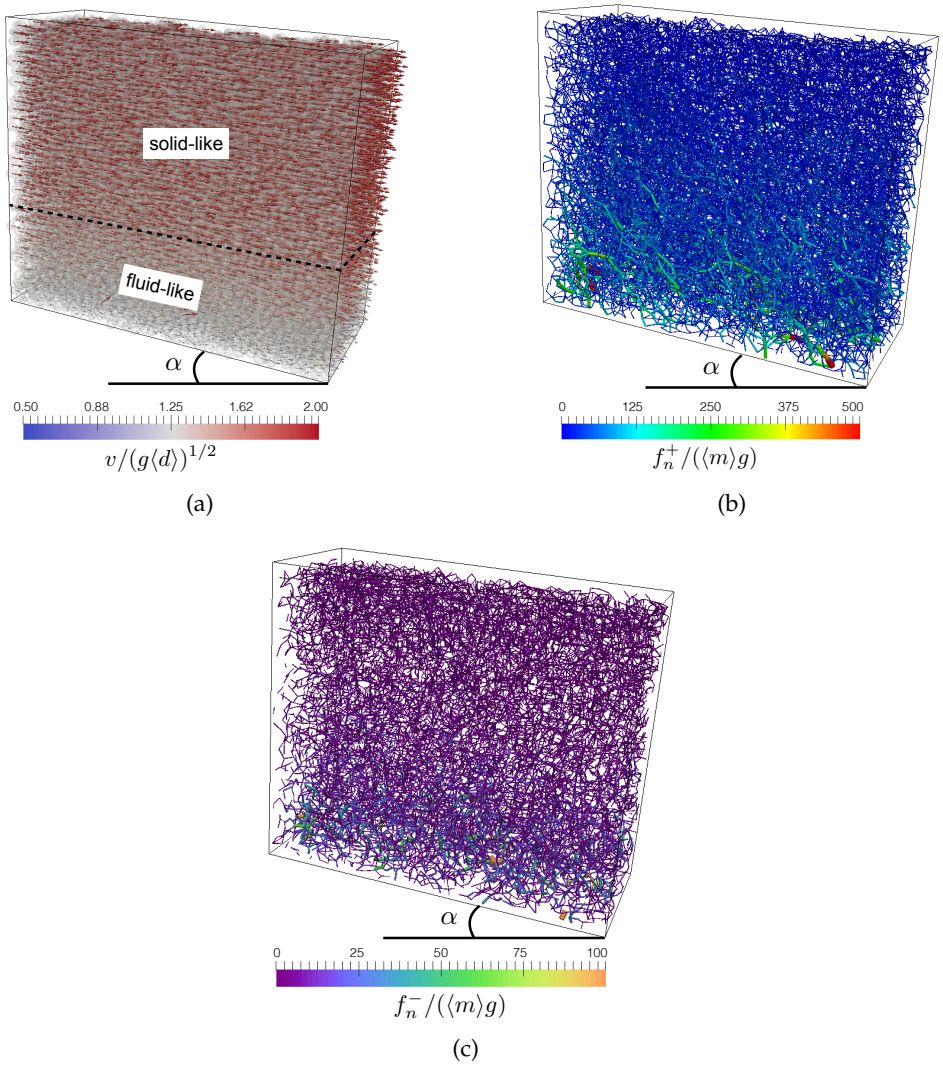

Fig. 4. (a) Particles' velocity of granular materials flow down on an inclined plane in the solid-like and fluid-like regions, the normal compressive (b) and tensile (c) forces distribution for the case of the inclination angle $\alpha = 23$ deg. in the steady-flowing state. The color maps represent the particles velocity magnitude and size of compressive and tensile forces, respectively. The forces are shown as lines joining the centers of two particles in capillary contacts, and the lines' thickness reveals the magnitude of the forces

To clarify the flowability of wet granular flow on an inclined plane in its steady-flowing state, the velocity profiles are studied. Fig. 4(a) displays the snapshot of the separation of the solid-like and fluid-like regions during the flows. All particles' velocities are almost the same in the solid-like layer, whereas the particle velocity decreases

proportionally to the depth of the sample in the fluid-like layer. This stability and variation of the particle velocity in both layers are analyzed in detail via the velocity profiles and the solid fraction. Figs. 5(a) and (b) show the velocity profiles and packing fraction along with the height of the sample for three different values of the inclination angle with a given value of the cohesion stress and the liquid viscosity in the steady-state, respectively. It is interesting to see that the solid-like and fluid-like layers appear for all cases of the inclination angle but in different thicknesses and velocities. For the case of $\alpha = 23$ deg., the normalized velocity at the free surface is about 1.9, this ratio increases rapidly to about 4.1 for $\alpha = 25$ deg. and approximate 6.4 for $\alpha = 27$ deg., as shown in Fig. 5(a). Thus, the increase of the inclination angle α strongly enhances the mobility of the wet granular flows, this was also shown in Fig. 3(a).

Due to the enhancement of the mobility of granular flows, the thickness of the solid-like layers decreases with an increase of the inclination angle α. In particular, this thickness is about two-thirds of the sample height for $\alpha = 23$ deg., but decreases to approximately one-third for $\alpha = 25$ deg. and about one-fifth for $\alpha = 27$ deg., respectively. In other words, the increase of α leads to the strong development of fluid-like flows. In contrast to the separation of two different layers along with the height of the flows, the packing fractions Φ are nearly the same except for the layers closed to the free surface and inclined rough wall.

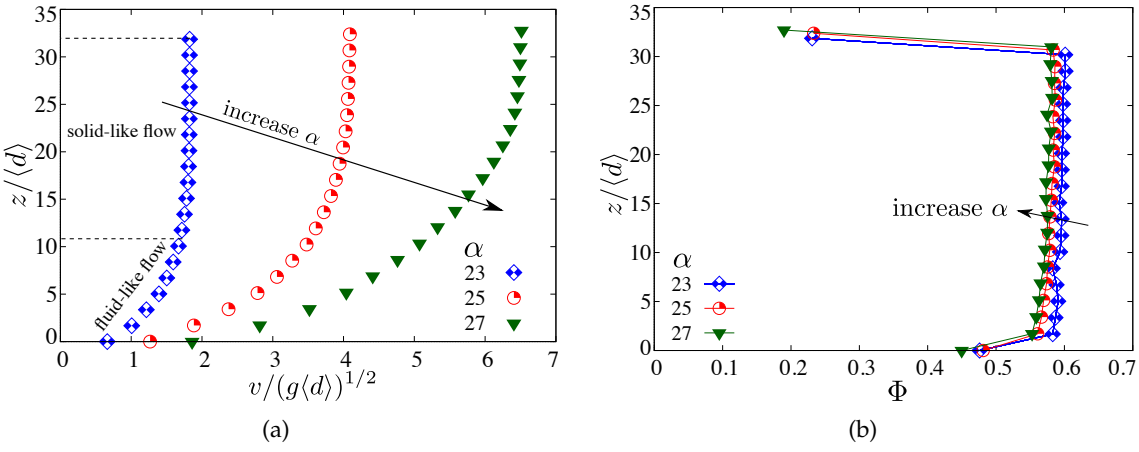

Fig. 5. (a) Velocity profile v and (b) the solid fraction Φ of wet granular materials in its steady-flowing state for different values of the inclination angle α

3.2. Force distribution

The flowability of the solid-like and fluid-like flows of wet granular materials on an inclined plane is associated with the force network established from the interactions between near-neighboring particles. This force network can be characterized by the normal forces and the tangential contact forces. Due to the contraction and extension properties of the capillary bridges between particles, the normal forces involve two different components (i.e. compressive and tensile forces) [41]. Meanwhile, the compressive forces tend to bind the particles together, the tensile forces tend to separate them. Figs. 4(b) and (c) display the snapshots of the normalized compressive forces f_n^+ network and the tensile forces f_n^- by the mean particle weight, respectively, for the case of $\alpha = 23$ deg. in the steady-flowing state of wet granular flow. It is remarkable to note that the force distribution of compressive and tensile components represents the significant differences between the solid-like layers and the fluid-like flows. In particular, the intensity of both f_n^+ and f_n^- for the solid-like layer is nearly constant due to the inherent properties of the capillary bonds formed between near-neighboring particles, whereas the values of f_n^+ and f_n^- in the fluid-like flows vary in a broad range depending on the collision and relative velocity between these grains.

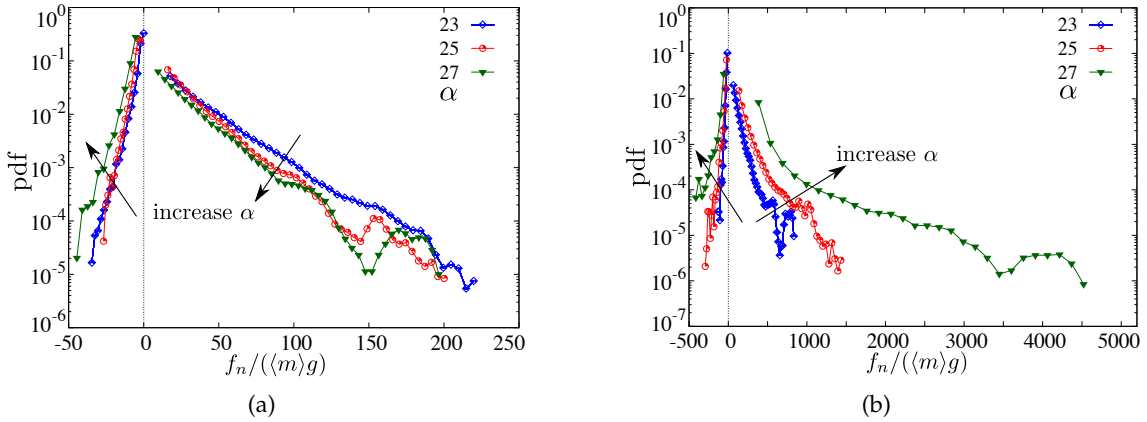

Fig. 6. Probability density function (pdf) of the normal compressive f_n^+ and tensile f_n^- forces for the solid-like flows (a) and fluid-like flows (b) of wet granular materials on an inclined plane with three different values of the inclination angle α

In order to get a better understanding of the force distribution in the solid-like and fluid-like flows, the probability density function (pdf) of the normal and tangential forces are considered. Figs. 6(a) and (b) display the pdfs of the normal tensile forces and normal compressive forces normalized by the mean particle weight for three different values of the inclination angle α for the solid-like layers and fluid-like flows, respectively. These

pdfs are divided into the positive and negative range at $f_n/(\langle m \rangle g) = 0$. For the negative range, meanwhile, the intensity of the tensile forces for the fluid-like flows is nearly 10 times as compared to the solid-like layers, the density of the tensile forces for the solid-like is slightly higher than that of the fluid-like regions. Furthermore, in contrast to the same effects of the inclination angle on the tensile forces in both solid-like and fluid-like layers, the increase of α leads to the slight decrease in the intensity of the compressive forces in solid-like flows, but this positive range significantly increases with increasing of α, this can be explained due to the strong collision between particles in the system with strong mobility.

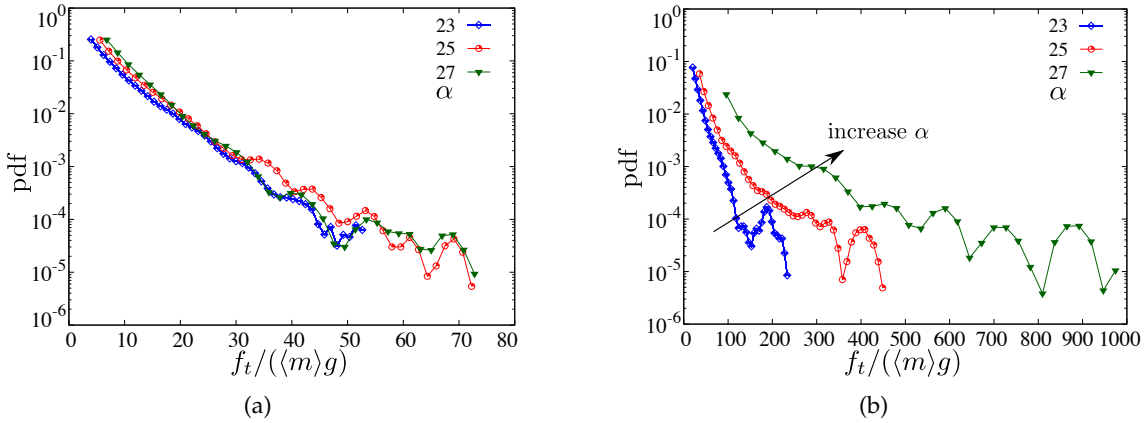

Fig. 7. Probability density function (pdf) of the normalized tangential forces f_t by the mean particle weight ($\langle m \rangle g$) for the solid-like region (a) and fluid-like region (b) of wet granular flows on an inclined plane with three different values of the inclination angle α

Although the observations above highlighted the flowability of the gravity-driven wet granular flows which are partly characterized by the different effects of the inclination angle of the plane on the distribution of the normal compressive forces and normal tensile forces, it is essential to check the probability density function of the tangential forces. Figs. 7(a) and (b) show the pdfs of the tangential force f_t normalized by the mean particle weight for three different values of the inclination angle of both solid-like layers and fluid-like flows of wet granular materials. Similar to the compressive forces of the fluid-like regions of granular flows, the intensity of the tangential forces significantly increases with increasing of the inclination angle α, as shown in Fig. 7(b). In particular, the normalized strongest tangential force is approximate 200 for the case with $\alpha = 23$ deg., this increases up to 480 for $\alpha = 25$ deg. and approximately 1000 for $\alpha = 27$ deg., respectively. These increases may be explained due to the high mobility of granular materials and the large relative tangential displacements between grains in the fluid-like flows. These explanations are clearly evidenced by the same distribution of the frictional forces

as a consequence of nearly no local shear strain rate between particles in the solid-like layers for three different values of α.

4. CONCLUTIONS

In this paper, we used an extensive three-dimensional discrete element method to analyze the effects of the inclination angle on the flowability of gravity-driven wet granular free-surface flows. The classical-numerical method with the approximate analytical expressions of the capillary cohesion forces and viscous forces induced by the capillary bonds between grains. In our simulations, the capillary bridges and the particle size are assumed to be distributed homogeneously, and each capillary bond can be reformed after breaking, this physical assumption is approximate to the reformation of the liquid bridges in nature. During the flowing of wet granular materials down an inclined plane, the granular flows separate into the solid-like region and the fluid-like layer. The depth of these regions strongly depends on the inclination angle of the plane.

As reported in the paper, the flowability of the gravity-driven wet granular free-surface flows can be characterized by the velocity profiles and the probability density functions of the normal forces (including the tensile and compressive components) and the tangential forces in both solid-like and fluid-like regions. We showed that the inclination angle of the plane strongly governs the mobility of wet granular flows as a consequence of keeping the roughness of the plane surface, leading to the increase of the velocity on the free surface of the sample as well as increasing the depth of the fluid-like flows. More interestingly, the increase of the inclination angle leads to the increase of both density and width of the compressive and tensile components of the normal forces and the tangential forces of the fluid-like regions, whereas there is a small effect on the normal tensile and compressive forces in the solid-like layers. These results highlight the behavior of the solid-like and fluid-like flows that occurred in the gravity-driven wet granular free-surface flows.

ACKNOWLEDGMENT

This research is funded by Danang Architecture University under grant number KTD-2021-02.

REFERENCES

[1] O. Pouliquen. Scaling laws in granular flows down rough inclined planes. *Physics of Fluids*, **11**, (3), (1999), pp. 542–548. https://doi.org/10.1063/1.869928.

[2] O. Pouliquen. Velocity correlations in dense granular flows. *Physical Review Letters*, **93**, (2004). https://doi.org/10.1103/physrevlett.93.248001.

[3] C. Zhu, Y. Huang, and J. Sun. Solid-like and liquid-like granular flows on inclined surfaces under vibration–Implications for earthquake-induced landslides. *Computers and Geotechnics*, **123**, (2020). https://doi.org/10.1016/j.compgeo.2020.103598.

[4] D. Ertaş and T. C. Halsey. Granular gravitational collapse and chute flow. *Europhysics Letters (EPL)*, **60**, (2002), pp. 931–937. https://doi.org/10.1209/epl/i2002-00307-8.

[5] C. Goujon, N. Thomas, and B. Dalloz-Dubrujeaud. Monodisperse dry granular flows on inclined planes: Role of roughness. *The European Physical Journal E*, **11**, (2003), pp. 147–157. https://doi.org/10.1140/epje/i2003-10012-0.

[6] M. Y. Louge. Model for dense granular flows down bumpy inclines. *Physical Review E*, **67**, (2003). https://doi.org/10.1103/physreve.67.061303.

[7] C. Cassar, M. Nicolas, and O. Pouliquen. Submarine granular flows down inclined planes. *Physics of Fluids*, **17**, (10), (2005). https://doi.org/10.1063/1.2069864.

[8] T. Börzsönyi and R. E. Ecke. Flow rule of dense granular flows down a rough incline. *Physical Review E*, **76**, (3), (2007). https://doi.org/10.1103/physreve.76.031301.

[9] R. Delannay, M. Louge, P. Richard, N. Taberlet, and A. Valance. Towards a theoretical picture of dense granular flows down inclines. *Nature Materials*, **6**, (2007), pp. 99–108. https://doi.org/10.1038/nmat1813.

[10] GDR-MiDi. On dense granular flows. *The European Physical Journal E*, **14**, (2004), pp. 341–365. https://doi.org/10.1140/epje/i2003-10153-0.

[11] O. Pouliquen, C. Cassar, P. Jop, Y. Forterre, and M. Nicolas. Flow of dense granular material: towards simple constitutive laws. *Journal of Statistical Mechanics: Theory and Experiment*, **2006**, (07), (2006). https://doi.org/10.1088/1742-5468/2006/07/p07020.

[12] P. Jop, Y. Forterre, and O. Pouliquen. A constitutive law for dense granular flows. *Nature*, **441**, (2006), pp. 727–730. https://doi.org/10.1038/nature04801.

[13] L. E. Silbert, D. Ertaş, G. S. Grest, T. C. Halsey, D. Levine, and S. J. Plimpton. Granular flow down an inclined plane: Bagnold scaling and rheology. *Physical Review E*, **64**, (5), (2001). https://doi.org/10.1103/physreve.64.051302.

[14] Y. Zhang and C. S. Campbell. The interface between fluid-like and solid-like behaviour in two-dimensional granular flows. *Journal of Fluid Mechanics*, **237**, (1992), pp. 541–568. https://doi.org/10.1017/s0022112092003525.

[15] P. G. Rognon, J.-N. Roux, M. Naaim, and F. Chevoir. Dense flows of cohesive granular materials. *Journal of Fluid Mechanics*, **596**, (2008), pp. 21–47. https://doi.org/10.1017/s0022112007009329.

[16] S. Mandal, M. Nicolas, and O. Pouliquen. Insights into the rheology of cohesive granular media. *Proceedings of the National Academy of Sciences*, **117**, (2020), pp. 8366–8373. https://doi.org/10.1073/pnas.1921778117.

[17] H. Moharamkhani, R. Sepehrinia, M. Taheri, M. Jalalvand, M. Brinkmann, and S. M. Vaez Allaei. Ordered/disordered monodisperse dense granular flow down an inclined plane: dry versus wet media in the capillary bridge regime. *Granular Matter*, **23**, (3), (2021), pp. 1–16. https://doi.org/10.1007/s10035-021-01115-4.

[18] R. Brewster, G. S. Grest, J. W. Landry, and A. J. Levine. Plug flow and the breakdown of Bagnold scaling in cohesive granular flows. *Physical Review E*, **72**, (6), (2005). https://doi.org/10.1103/physreve.72.061301.

[19] L. E. Silbert, J. W. Landry, and G. S. Grest. Granular flow down a rough inclined plane: Transition between thin and thick piles. *Physics of Fluids*, **15**, (2003), pp. 1–10. https://doi.org/10.1063/1.1521719.

[20] S. H. Chou and S. S. Hsiau. Experimental analysis of the dynamic properties of wet granular matter in a rotating drum. *Powder Technology*, **214**, (2011), pp. 491–499. https://doi.org/10.1016/j.powtec.2011.09.010.

[21] P. A. Cundall and O. D. L. Strack. A discrete numerical model for granular assemblies. *Géotechnique*, **29**, (1979), pp. 47–65. https://doi.org/10.1680/geot.1979.29.1.47.

[22] F. Radjai and F. Dubois. *Discrete-element modeling of granular materials*. Wiley-Iste, (2011).

[23] T.-T. Vo. Rheology and granular texture of viscoinertial simple shear flows. *Journal of Rheology*, **64**, (5), (2020), pp. 1133–1145. https://doi.org/10.1122/8.0000033.

[24] S. Luding. Collisions & contacts between two particles. In *Physics of dry granular media*, pp. 285–304. Springer, (1998).

[25] H. J. Herrmann and S. Luding. Modeling granular media on the computer. *Continuum Mechanics and Thermodynamics*, **10**, (1998), pp. 189–231. https://doi.org/10.1007/s001610050089.

[26] T.-T. Vo, T. L. Vu, and P. Mutabaruka. Effects of size polydispersity on segregation of spherical particles in rotating drum. *The European Physical Journal E*, **44**, (6), (2021), pp. 1–10. https://doi.org/10.1140/epje/s10189-021-00091-0.

[27] V. Richefeu, M. S. E. Youssoufi, R. Peyroux, and F. Radjaï. A model of capillary cohesion for numerical simulations of 3D polydisperse granular media. *International Journal for Numerical and Analytical Methods in Geomechanics*, **32**, (2008), pp. 1365–1383. https://doi.org/10.1002/nag.674.

[28] T.-T. Vo. Erosion dynamics of wet particle agglomerates. *Computational Particle Mechanics*, **8**, (3), (2021), pp. 601–612. https://doi.org/10.1007/s40571-020-00357-y.

[29] J. Duran, A. Reisinger, and P. de Gennes. *Sands, powders, and grains: an introduction to the physics of granular materials*. Partially Ordered Systems, Springer New York, (1999).

[30] T. T. Vo, S. Nezamabadi, P. Mutabaruka, J.-Y. Delenne, and F. Radjai. Additive rheology of complex granular flows. *Nature Communications*, **11**, (1), (2020), pp. 1–8. https://doi.org/10.1038/s41467-020-15263-3.

[31] J. Shäfer, S. Dippel, and D. E. Wolf. Force schemes in simulations of granular materials. *Journal de Physique I*, **6**, (1996), pp. 5–20. https://doi.org/10.1051/jp1:1996129.

[32] T. K. Nguyen, A. A. Claramunt, D. Caillerie, G. Combe, S. D. Pont, J. Desrues, and V. Richefeu. FEM $\times$ DEM: a new efficient multi-scale approach for geotechnical problems with strain localization. *EPJ Web of Conferences*, **140**, (2017). https://doi.org/10.1051/epjconf/201714011007.

[33] T.-T. Vo, C. T. Nguyen, T.-K. Nguyen, V. M. Nguyen, and T. L. Vu. Impact dynamics and power-law scaling behavior of wet agglomerates. *Computational Particle Mechanics*, **9**, (3), (2022), pp. 537–550. https://doi.org/10.1007/s40571-021-00427-9.

[34] C. M. Donahue, C. M. Hrenya, and R. H. Davis. Stokes's cradle: Newton's cradle with liquid coating. *Physical review letters*, **105**, (3), (2010). https://doi.org/10.1103/physrevlett.105.034501.

[35] C. M. Donahue, R. H. Davis, A. A. Kantak, and C. M. Hrenya. Mechanisms for agglomeration and deagglomeration following oblique collisions of wet particles. *Physical Review E*, **86**, (2), (2012). https://doi.org/10.1103/physreve.86.021303.

[36] T. Mikami, H. Kamiya, and M. Horio. Numerical simulation of cohesive powder behavior in a fluidized bed. *Chemical Engineering Science*, **53**, (1998), pp. 1927–1940. https://doi.org/10.1016/s0009-2509(97)00325-4.

[37] G. Lian, C. Thornton, and M. J. Adams. A theoretical study of the liquid bridge forces between two rigid spherical bodies. *Journal of Colloid and Interface Science*, **161**, (1993), pp. 138–147. https://doi.org/10.1006/jcis.1993.1452.

[38] V. Richefeu, F. Radjaı, and M. S. El Youssoufi. Stress transmission in wet granular materials. *The European Physical Journal E*, **21**, (4), (2006), pp. 359–369. https://doi.org/10.1140/epje/i2006-10077-1.

[39] V. Richefeu, M. S. El Youssoufi, and F. Radjai. Shear strength properties of wet granular materials. *Physical Review E*, **73**, (5), (2006). https://doi.org/10.1103/physreve.73.051304.

[40] J. Happel and H. Brenner. *Low Reynolds number hydrodynamics*. Martinus Nijhoff Publishers, The Hague, the Netherlands, (1983).

[41] T.-T. Vo and C. T. Nguyen. Characteristics of force transmission in cohesive agglomerates impacting a rigid surface. *Mechanics Research Communications*, **117**, (2021). https://doi.org/10.1016/j.mechrescom.2021.103773.